
TempLe: Learning Template of Transitions for Sample Efficient Multi-task RL

Yanchao Sun¹ Xiangyu Yin² Furong Huang¹

Abstract

Transferring knowledge among various environments is important to efficiently learn multiple tasks online. Most existing methods directly use the previously learned models or previously learned optimal policies to learn new tasks. However, these methods may be inefficient when the underlying models or optimal policies are substantially different across tasks. In this paper, we propose Template Learning (TempLe), the first PAC-MDP method for multi-task reinforcement learning that could be applied to tasks with varying state/action space. TempLe generates transition dynamics templates, abstractions of the transition dynamics across tasks, to gain sample efficiency by extracting similarities between tasks even when their underlying models or optimal policies have limited commonalities. We present two algorithms for an “online” and a “finite-model” setting respectively. We prove that our proposed TempLe algorithms achieve much lower sample complexity than single-task learners or state-of-the-art multi-task methods. We show via systematically designed experiments that our TempLe method universally outperforms the state-of-the-art multi-task methods (PAC-MDP or not) in various settings and regimes.

1. Introduction

Multi-task reinforcement learning (MTRL) (Wilson et al., 2007; Brunskill & Li, 2013; Modi et al., 2018) requires the agent to efficiently tackle a series of tasks. A key goal of MTRL is to improve per-task learning efficiency compared against single-task learners, by using the knowledge obtained from previous tasks to learn new tasks.

Despite the recent rapid progress in MTRL, some issues remain unsettled. (1) *Guaranteed sample efficiency*. Only a few existing methods have guarantees on sample efficiency,

the most common bottleneck of RL algorithms. (2) *Correctness v.s. efficiency*. An overly aggressive application of previous knowledge may transfer incorrect knowledge and deteriorate the performance on new tasks, resulting in a “negative transfer” (Taylor & Stone, 2009). However, if an agent is overly conservative in applying previously learned knowledge, much of the similarities between tasks will be ignored, resulting in an “inefficient transfer”. It is nontrivial to balance between the correctness and efficiency or achieve both. (3) *Varying state/action space across tasks*. In practice, transferring knowledge learned from smaller environments to learning in larger environments is extremely useful. However, most existing works on MTRL assume the state/action space is shared across tasks.

In an effort to provide guaranteed sample efficiency for MTRL, Brunskill & Li (2013) propose the first PAC-MDP¹ algorithm which clusters the underlying MDP models of the tasks into groups and identifies new tasks as learned groups. However, transferring knowledge from the clustered underlying MDPs could be an “inefficient transfer” if the underlying MDPs are too different to be clustered into a small number of groups. Similarly, in some other model-based approaches (Liu et al., 2016; Modi et al., 2018), only the similarities of underlying MDP models are exploited to characterize the similarities across the tasks.

We remedy the aforementioned “inefficient transfer” problem using the prior knowledge learned from the *state-action transition dynamics* (the transition probability combined with its reward for a state-action pair), allowing extraction of more commonalities in tasks without suffering from “negative transfer”. A motivating example is the navigation problem in mazes with slippery floors, where an agent aims to reach an objective state/location in a maze with 4 actions: go up, down, left and right. The slipperiness of the floor, which makes the transition dynamics stochastic, depends on the landform of the location, such as sand, marble and ice. Different landforms have different transition dynamics, although the same landforms share the transition dynamics. Consider a $\sqrt{S} \times \sqrt{S}$ maze with G types of landforms. We show in Figure 1 some examples of different combina-

¹Department of Computer Science, University of Maryland, College Park, MD ²Beijing University of Posts and Telecommunications, China. Correspondence to: Furong Huang <furongh@cs.umd.edu>.

¹An algorithm is PAC-MDP (Probably Approximately Correct in Markov Decision Processes) if its sample complexity is polynomial in the environment size and approximation parameters with high probability.

tions/distributions of the landforms in the maze. The number of underlying MDP models could be up to G^S , making it prohibitive to extract similarities from the models. However, the types of underlying transition dynamics associated with each state/location are governed by the number of distinct landforms G . With this idea, we transfer knowledge from sand to sand, marble to marble, and ice to ice. Therefore, we achieve more effective and efficient knowledge transfer by similarities at the level of *state-action transition dynamics* instead of MDP *model dynamics*. More importantly, we can extend the knowledge learned from a $\sqrt{S} \times \sqrt{S}$ maze to any-sized mazes consisting of these same types of landforms (such as Figure 1d). The challenge of learning is now reduced to extracting such “landforms” without prior knowledge of the tasks.

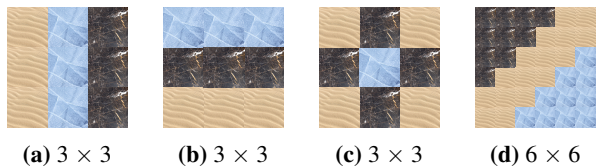


Figure 1. Examples of landform combinations, where  stands for sand,  stands for marble and  stands for ice.

Motivated by the ideas above, we propose a novel method called *Template Learning (TempLe)* for MTRL, which provably guarantees sample efficiency and achieves efficient transfer learning for multi-task reinforcement learning with varying state/action space. We extract templates for similar state-action transition dynamics (landforms in the example above), called *Transition Templates*, and confidently improve the efficiency of transition dynamics estimation in new tasks. By sharing experience among state-action pairs associated with similar templates, the learning process is expedited. We introduce two versions of TempLe: one is for online MTRL without prior knowledge about models, named *Online Template Learning (O-TempLe)*, the other further improves the learning efficiency based on a finite model assumption, named *Finite-Model Template Learning (FM-TempLe)*.

Summary of Contributions: (1) Our proposed method achieves a significant *reduction of sample complexity* compared with state-of-the-art PAC-MDP algorithms. The sample complexity is only linearly dependent on the number of states and the number of templates, when high precision is desired. (2) Our algorithms cover two complementary settings, solving MTRL problems in different regimes – *with or without prior knowledge of models*. (3) To the best of our knowledge, what we propose is the *first PAC-MDP algorithm* that is able to learn tasks with *varying state/action spaces*.

2. Related Work

Empirical Studies. MTRL/lifelong RL and *Transfer Learning (TL)* (Torrey & Shavlik, 2010) are closely related, and have been studied for years. Taylor & Stone (2009) survey a wide range of empirical results on transferring knowledge among tasks, and point out some problems of previous works, including negative transfer, partially due to the lack of theoretical analysis.

PAC-MDP Algorithms. Brunskill & Li (2013) present the first formal analysis of the sample complexity for MTRL. They propose a two-phase algorithm and prove that per-task sample complexity is reduced compared with single-task learners. However, they require all tasks coming from a small number of models, and when the number of distinct models is large, their algorithm becomes comparable with single-task learning. In this paper, we show our proposed methods outperform the method provided by Brunskill & Li (2013) both in theory and in experiments.

There are other PAC-MDP algorithms for multi-task RL, considering the problem from different perspectives. For example, Brunskill & Li (2014) discuss lifelong learning in semi-Markov decision processes (SMDPs), where options are involved. Liu et al. (2016) extend the finite-model method (Brunskill & Li, 2013) to continuous state space. Modi et al. (2018) improve the learning efficiency through the assistance of side informations.

Non-PAC Algorithms. Besides the above methods with PAC guarantees, there are many interesting approaches aiming to effectively transfer knowledge across tasks. Some approaches augment the learning of a new task by reusing the policies learned from previous tasks (Ramamoorthy et al., 2013; Li & Zhang, 2018), though a library of reliable source policies is usually needed. The hierarchical multi-task learning algorithm proposed by Wilson et al. (2007) learns a Bayesian mixture model from previous tasks, and use the learned distribution as a prior of new tasks. Although good experimental results are shown, there are no theoretical guarantees. Abel et al. (2018) introduce two types of state-abstractions that can reduce the problem complexity and improve the learning of new tasks. However, as shown in the paper, the proposed abstractions, when combined with PAC-MDP algorithms such as RMax (Brafman & Tennenholtz, 2003), the PAC guarantee does not hold anymore and the number of mistakes made by the agent can be arbitrarily large. In this paper, we show our proposed method outperforms the abstraction method empirically.

Cross-Domain Learning. Knowledge transfer between tasks with various state/action spaces (task domains) is also an important topic. As summarized by Taylor & Stone (2009), most early works require hand-coded inter-task mappings (Taylor & Stone, 2007), or only learn from unchanged

problem representations (Konidaris & Barto, 2006; Sharma et al., 2007). Recently, Ammar et al. (2015) propose an algorithm that can perform cross-domain transfer efficiently. The authors assume tasks are from a finite set of domains, and parametrize each task’s policy by the product of a shared knowledge base and task-specific coefficients. However, although convergence guarantee is provided, there is no guarantee for sample efficiency.

3. Preliminaries and Notations

For the learning of a single task, an agent interacts with the environment described by a Markov Decision Process (MDP). In this paper, we focus on discrete and finite MDPs defined as a tuple $\langle \mathcal{S}, \mathcal{A}, p(\cdot|\cdot, \cdot), r(\cdot, \cdot), \mu, \gamma \rangle$, where \mathcal{S} is the state space (with cardinality S); \mathcal{A} is the action space (with cardinality A); $p(\cdot|\cdot, \cdot)$ is the transition probability function with $p(s'|s, a)$ representing the probability of transitioning to state s' from state s by taking action a ; $r(\cdot, \cdot)$ is the reward function with $r(s, a)$ recording the reward achieved by taking action a in state s ; μ is the initial state distribution; γ is the discount factor. $p(\cdot|\cdot, \cdot)$ and $r(\cdot, \cdot)$ together are called the **model dynamics** of the MDP. Denote the maximum value of r as R_{max} .

At every step, the agent selects an action based on the current *policy* π . The value function of a policy $V^\pi(s)$, which evaluates the performance of a policy π , is the expected average reward gained by following π starting from s . Similarly, the action value $Q^\pi(s, a)$ is the expected average reward starting from pair (s, a) . In an RL task, an agent searches for the optimal policy by interacting with the MDP. We use V_{max} to denote the upper bound of V . In the discounted setting $V_{max} = \frac{R_{max}}{1-\gamma}$.

The general goal of RL algorithms is to learn the optimal policy for an MDP with as few interactions as possible. For any $\epsilon > 0$ and any step $h > 0$, if the policy π_h generated by an RL algorithm L satisfies $V^* - V^{\pi_h} \leq \epsilon$, we say L is near-optimal at step h . If for any $0 < \delta < 1$, the total number of steps that L is not near-optimal is upper bounded by a function $\zeta(\epsilon, \delta)$ with probability at least $1 - \delta$, then ζ is called the *sample complexity* (Kakade et al., 2003) of L .

4. Learning with Templates

As motivated in the example described in Section 1, the main idea of this work is to boost the learning process by aggregating similar state-action transition dynamics. We permute the elements of transition dynamics/probability vectors to be in descending order, and aggregate these permuted transition probabilities to obtain “templates of transition” which will be defined in Definition 2. We show that the templates are effective abstractions of the environment.

We introduce our proposed Template Learning (TempLe) method in this section. Our settings of multi-task learning are stated in Section 4.1. Then, we formally define Transition Template (TT) and some key concepts in Section 4.2 and explain how they are used in practice in Section 4.3. Section 4.4 proposes an online algorithm named O-TempLe, and Section 4.5 introduces FM-TempLe, a more efficient algorithm based on a finite model assumption.

4.1. Two Settings: Online vs Finite-Model MTRL

Online MTRL. In this work, we focus on online multi-task learning, where an agent interacts with multiple tasks streaming-in, each of which is corresponding to a specific MDP. The tasks are i.i.d. drawn from a set \mathcal{M} of MDPs (models). MDPs in \mathcal{M} may have different dynamics or state/action space. The number of MDPs in the set $|\mathcal{M}|$ can be very large or infinite. The learning process is: for $t = 1, 2, \dots$, the agent (1) receives a new task $M_t \in \mathcal{M}$, (2) chooses a policy π_t , and (3) experiences M_t till the end of the task.

Finite-Model MTRL. Similarly with online MTRL, in finite-model MTRL, the agent still interacts with streaming-in tasks drawn from a set \mathcal{M} of MDPs. However, the number of MDPs in the set $|\mathcal{M}|$ should be finite and not large.

Online MTRL is a more realistic setting, requiring no prior knowledge of the types of underlying MDPs. Finite-model MTRL assumes small types of MDPs, which could potentially allow more efficient learning.

4.2. Transition Template: An Abstraction of Dynamics

In this section, we introduce a more compact way to represent the model dynamics of an MDP. We first formally define the transition dynamics of a state-action (s-a) pair.

Definition 1 (State-Action (s-a) Transition Dynamics). *For any state-action pair (s, a) , its **transition dynamics** is defined as a length- $(S + 1)$ vector $\theta(s, a) = [p(s_1|s, a), p(s_2|s, a), \dots, p(s_S|s, a), r(s, a)]$.*

Note that s-a transition dynamics are different from the model dynamics, which characterize the transitions for all s-a pairs. In s-a transition dynamics, the first S elements form the transition probability vector $p(\cdot|s, a)$. As defined in most RL literatures (Kakade et al., 2003; Brunskill & Li, 2013), the order of elements in $p(\cdot|s, a)$ is the natural order of the states.

In contrast, we propose to re-order the elements of $p(\cdot|s, a)$ by their values, and obtain a more compact representation of the transition dynamics called *Transition Template*.

Definition 2 (Transition Template). *A **Transition Template** (TT) \mathbf{g} is defined as a tuple $(\mathbf{g}^{(p)}, \mathbf{g}^{(r)})$, where $\mathbf{g}^{(p)} \in \mathbb{R}^l$ is a transition probability vector with non-increasingly ordered*

elements, i.e., $\sum_{i=1}^l g_i^{(p)} = 1$ and $g_i^{(p)} \geq g_j^{(p)}, \forall 1 \leq i \leq j \leq l$; $g^{(r)} \in R$ is a scalar representing the reward.

Any s-a transition dynamics can be permuted to a unique TT by re-arranging the transition probability vector $p(\cdot|s, a)$ in a decreasing order and maintaining the reward $r(s, a)$ to $g^{(r)}$, i.e., $\mathbf{g}_{(s,a)} = (\text{desc}(p(\cdot|s, a)), r(s, a))$, where desc orders the elements of $p(\cdot|s, a)$ from the largest value to the smallest value. For example, if $\theta(s_1, a_1) = [0.3, 0.7, 0, 1]$, and $\theta(s_2, a_2) = [0, 0.3, 0.7, 1]$, then (s_1, a_1) and (s_2, a_2) have the same TT $([0.7, 0.3, 0], 1)$, although their s-a transition dynamics are different.

A TT is a representation of s-a transition dynamics with some similarities. It ignores how the s-a pair transits to a specific next state, but only considers the patterns of transition probabilities, allowing more efficient exploitation of similarities. An intuitive example is given in Figure 2, where there are 100 distinct s-a transition dynamics, but only 2 distinct TTs.

The distance between two different TTs is defined as the ℓ_2 distance between $\mathbf{g}^{(p)}$'s plus the absolute difference between $g^{(r)}$'s. See Definition 5 Appendix A for more details.

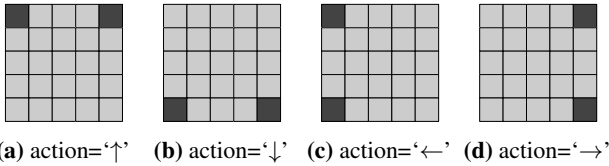


Figure 2. An example of TTs in a 5×5 slippery gridworld with no reward and slipping probability=0.4. The template at all \blacksquare s is $\mathbf{g}_1 = ([0.8, 0.2, 0, \dots, 0], 0)$, and the template at all \blacksquare s is $\mathbf{g}_2 = ([0.6, 0.2, 0.2, 0, \dots, 0], 0)$.

4.3. Empirical Estimation of Transition Templates

Section 4.2 defines TT based on the underlying s-a transition dynamics. However, in reality, we do not have access to the underlying dynamics. In model-based RL, a key step is to estimate the dynamics and to build a model of the environment. We now illustrate the estimate of TTs, as well as how TTs augments the learning process.

The conventional estimation of s-a transition dynamics.

A direct estimation of $\theta(s, a)$ is obtained through experience $\hat{\theta}(s, a) = [\frac{n(s,a,s_1)}{n(s,a)}, \frac{n(s,a,s_2)}{n(s,a)}, \dots, \frac{n(s,a,s_S)}{n(s,a)}, \frac{R(s,a)}{n(s,a)}]$, where $n(s, a, s')$ is the number of observations of transitioning from s to s' by taking action a , $n(s, a)$ is the total number of observations of (s, a) , and $R(s, a)$ is the cumulative rewards obtained by (s, a) . An accurate estimation of the transition dynamics $\theta(s, a)$ requires a large enough number of observations $n(s, a)$ according to the theory of concentration bounds. Therefore, it is sample-consuming to accurately estimate the transition dynamics of every s-a pair by the estimation above.

Augmented estimation of s-a transition dynamics. As discussed in Section 4.2, different s-a pairs may share the same TTs. Our goal is then to aggregate the estimations of s-a transition dynamics associated with the same TTs. We introduce the following process to obtain estimations of all s-a transition dynamics:

- (1) *rough estimation*: obtain $\hat{\theta}(s, a) = n(s, a, \cdot)/n(s, a)$ for each (s, a) with a small n ;
- (2) *permutation*: permute each $\hat{\theta}(s, a)$ to its corresponding permuted estimates $\hat{\mathbf{g}}_{(s,a)}$
- (3) *template identification*: identify the group of the permuted estimate $\hat{\mathbf{g}}_{(s,a)}$ such that permuted estimates are similar within the group, and obtain a more confident estimation of TT $\hat{\mathbf{g}}$ aggregating within-group statistics.
- (4) *augmentation*: for every (s, a) , obtain a more confident estimation of the transition dynamics by permuting back its corresponding TT with accumulated knowledge.

The noisy estimate of transition dynamics will not render error other than the smaller amount of noise in estimated transition templates if it is identified into the right group. To guarantee accurate identification, the ordering of the elements in the noisy estimate should be consistent with the ground truth. Therefore, the consistency of our estimation depends on TT gap as defined in Definition 5 and ‘‘ranking gap’’ as defined in Definition 7 (see Appendix A for details). An example in Appendix B shows how augmented estimation helps save a large number of samples compared against the conventional estimation.

Now we are ready to formally introduce our algorithms in two settings respectively.

4.4. O-TempLe: Online Template Learning

The first algorithm we introduce is Online Template Learning (O-TempLe) for the online MTRL setting. O-TempLe is a meta learning algorithm with model-based ‘‘base learners’’ which compute policies for the current task. We illustrate O-TempLe in Procedure 1 using RMax (Brafman & Tennenholtz, 2003) as the base learner, and it can be replaced by other model-based methods such as E^3 (Kearns & Singh, 2002) and MBIE (Strehl & Littman, 2005).

The principle of RMax algorithm on an MDP M is to build an induced MDP based on a known threshold m . A state-action pair is said to be m -known if the number of visits/observations $n(s, a) \geq m$. A state is m -known if $n(s, a) \geq m, \forall a \in \mathcal{A}$. The set of all m -known states induces an MDP M_k , where for any m -known state s , $p(s'|s, a) = \frac{n(s,a,s')}{n(s,a)}$, $r(s, a) = \frac{R(s,a)}{n(s,a)}$ and for any non- m -known state s , $p(s'|s, a) = \mathbb{I}\{s' = s\}$, $r(s, a) = R_{\max}$. Then, RMax computes an optimal policy based on the optimistic model by dynamic programming.

In contrast, O-TempLe uses augmented estimation intro-

duced in Section 4.3 to reduce the required number of visits to every single s-a pair. Instead of aggregating the estimations of all s-a transition dynamics at once, O-TempLe asynchronously identifies the TTs of s-a pairs and updates the template groups in an online manner, through measuring the distances among TTs.

Procedure 1 Online Template Learning (O-TempLe)

Input: user-specified TT gap $\hat{\tau}$; error tolerance ϵ ; discount factor γ ; regular known threshold m ; small known threshold m_s

Output Near-optimal policies $\{\pi_t\}_{t=1,2,\dots}$

```

1: Initialize an empty TT group set  $\mathcal{G}$  and TT visit set  $\mathcal{O}$ 
2: for  $t \leftarrow 1, 2, \dots$  do
3:   Receive a task  $M_t$ ; initialize visits  $\mathbf{n}(s, a, \cdot) \leftarrow \mathbf{0}$ ,
    $R(s, a) \leftarrow 0, \forall (s, a) \in (\mathcal{S}, \mathcal{A})$ , an empty known state-
   action set  $\mathcal{K}$ , and a random policy  $\pi$ 
4:   for  $h \leftarrow 1, 2, \dots, H$  do
5:     ACT-AND-UPDATE( $s_h$ )
6:     if  $(s_h, a_h) \notin \mathcal{K}$  and  $\|\mathbf{n}(s_h, a_h, \cdot)\|_{\ell_1} = m_s$  then
7:        $\triangleright$  TT identification with the small threshold
8:        $\tilde{\mathbf{g}}, \mathbf{o}_{\tilde{\mathbf{g}}}, \sigma \leftarrow \text{GEN-TT}(\mathbf{n}(s_h, a_h, \cdot), R(s_h, a_h))$ 
9:       if no  $\mathbf{g} \in \mathcal{G}$  is  $\hat{\tau}$ -close to  $\tilde{\mathbf{g}}$  then
10:        Add  $\tilde{\mathbf{g}}$  to  $\mathcal{G}$ ,  $\mathbf{o}_{\tilde{\mathbf{g}}}$  to  $\mathcal{O}$ 
11:       else
12:        Find the closest TT  $\mathbf{g}^*$  to  $\tilde{\mathbf{g}}$ 
13:        TT-UPDATE( $\mathbf{g}^*, \mathbf{o}_{\mathbf{g}^*}, \mathbf{n}(s_h, a_h, \cdot), R(s_h, a_h)$ )
14:        AUGMENT( $\mathbf{o}_{\mathbf{g}^*}, \mathbf{n}(s_h, a_h, \cdot), R(s_h, a_h), \sigma$ )
15:       if  $(s_h, a_h) \notin \mathcal{K}$  and  $\|\mathbf{n}(s_h, a_h, \cdot)\|_{\ell_1} \geq m$  then
16:          $\triangleright$  policy update with the regular threshold
17:         Update  $\pi$  using visits  $\mathbf{n}$  and  $R$  by RMax
18:         Add  $(s_h, a_h)$  to  $\mathcal{K}$ 
19:       for all  $(s, a) \in (\mathcal{S}, \mathcal{A})$  with identified TT  $\mathbf{g}_{(s,a)}$  do
20:         TT-UPDATE( $\mathbf{g}_{(s,a)}, \mathbf{o}_{\mathbf{g}_{(s,a)}}, \mathbf{n}(s, a, \cdot), R(s, a)$ )
21: procedure ACT-AND-UPDATE( $s_h$ )
22:   Take action  $a_h \leftarrow \pi(s_h)$ , get  $s_{h+1}$  and  $r_h$ 
23:    $\mathbf{n}(s_h, a_h, s_{h+1}) \leftarrow \mathbf{n}(s_h, a_h, s_{h+1}) + 1$ 
24:    $R(s_h, a_h) \leftarrow R(s_h, a_h) + r_h$ 
    
```

Procedure 1 illustrates how O-TempLe works. In addition to the regular known threshold m used in RMax, we design a smaller known threshold m_s , which is the smallest number of visits to ensure identifying the TTs of all s-a pairs. If for any (s, a) , the total number of visits ($\|\mathbf{n}(s, a, \cdot)\|_{\ell_1}$) reaches m_s , then the TT of (s, a) will be identified by either creating a new TT and adding it to set \mathcal{G} (Line 8-10), or finding an existing TT within $\hat{\tau}$ -distance (Line 11-14). In the latter case, we synchronize the experience of (s, a) in the current task and the accumulated experience that its TT holds by calling functions TT-UPDATE and AUGMENT, which are given by Procedure 2. Accumulated experience of each TT is stored in a tuple $\mathbf{o}_{\mathbf{g}} = (\mathbf{o}_{\mathbf{g}}^{(N)}, \mathbf{o}_{\mathbf{g}}^{(R)})$, where $\mathbf{o}_{\mathbf{g}}^{(N)}$ is the total visits accumulated by permuted $\mathbf{n}(s, a, s')$ of all

(s, a) 's with TT \mathbf{g} . When (s, a) is m -known, the induced MDP is updated and a new policy is computed (Line 15-18). Overall, our O-TempLe allows s-a transition dynamics grouped together to share their visit counts, making it much easier for them to reach m visits than in regular RMax.

Note that Procedure 1 also works for tasks whose state/action space are different from tasks to task, since the comparison of TTs considers the non-zero elements of the transition vectors only. One can compute the difference between two different-size TTs by simply padding zeros to the end of the shorter TT.

Procedure 2 TT Functions

```

1: function GEN-TT( $\mathbf{n}, R$ )  $\triangleright$  generate TT
2:   find permutation  $\sigma$  s.t.  $\sigma(\mathbf{n})$  is in descending order
3:   ordered visits  $\mathbf{o}_{\mathbf{g}}^{(N)} \leftarrow \sigma(\mathbf{n}), \mathbf{o}_{\mathbf{g}}^{(R)} \leftarrow R, \mathbf{o}_{\mathbf{g}} \leftarrow (\mathbf{o}_{\mathbf{g}}^{(N)}, \mathbf{o}_{\mathbf{g}}^{(R)})$ 
4:   transition template  $\mathbf{g} \leftarrow (\frac{\mathbf{o}_{\mathbf{g}}^{(N)}}{\|\mathbf{n}\|_{\ell_1}}, \frac{\mathbf{o}_{\mathbf{g}}^{(R)}}{\|R\|_{\ell_1}})$ 
5:   return  $\mathbf{g}, \mathbf{o}_{\mathbf{g}}, \sigma$ 
6: function TT-UPDATE( $\mathbf{g}, \mathbf{o}_{\mathbf{g}}, \mathbf{n}, R$ )  $\triangleright$  add current visits to TT
7:    $\mathbf{o}_{\mathbf{g}} \leftarrow \mathbf{o}_{\mathbf{g}} + (\text{descending}(\mathbf{n}), R)$ 
8:    $\mathbf{g} \leftarrow (\frac{\mathbf{o}_{\mathbf{g}}^{(N)}}{\|\mathbf{o}_{\mathbf{g}}^{(N)}\|_{\ell_1}}, \frac{\mathbf{o}_{\mathbf{g}}^{(R)}}{\|\mathbf{o}_{\mathbf{g}}^{(R)}\|_{\ell_1}})$ 
9: function AUGMENT( $\mathbf{o}_{\mathbf{g}}, \mathbf{n}, R, \sigma$ )  $\triangleright$  augment visits by TT
10:   $\mathbf{n} \leftarrow \mathbf{n} + \sigma^{-1}(\mathbf{o}_{\mathbf{g}}^{(N)})$ 
11:   $R \leftarrow R + \mathbf{o}_{\mathbf{g}}^{(R)}$ 
    
```

4.5. FM-TempLe: Finite-Model Template Learning

Although Procedure 1 saves samples by accumulating knowledge within TT groups, the agent still needs to visit all s-a pairs before the model dynamics become known. This is natural for model-based algorithms. However, it is possible to get rid of the dependence on the size of state-action space, when the number of possible MDPs $|\mathcal{M}|$ is known and small. This idea, proposed by Brunskill & Li (2013), is called Finite-Model RL (FMRL), which makes this ‘‘finite model’’ assumption and achieves better sample complexity than single-task learners.

In this section, we propose Finite-Model Template Learning (FM-TempLe) in Procedure 3, which is based on O-TempLe, but further reduces sample complexity by making the same finite-model assumption as (Brunskill & Li, 2013). We will prove and verify that FM-TempLe outperforms FMRL.

In contrast with O-TempLe, FM-TempLe is able to correctly identify the TTs of some s-a pairs before they are visited for m_s times. This is because for a fixed MDP (model), how TTs are distributed over all s-a pairs is also fixed. If the number of underlying models is small, we can possibly obtain the TTs for all s-a pairs immediately after identifying the model.

FM-TempLe illustrated in Procedure 3 has two phases; the

first phase (tasks $1 - T_1$) collects models and the second phase (tasks $T_1 + 1, T_1 + 2, \dots$) identifies models. In Phase 1 (Line 2-3), the agent acts in the same way as O-TempLe in Procedure 1. At the end of Phase 1 (Line 4-5), the first T_1 tasks are clustered into finite groups of models. Then, in Phase 2 (Line 6-17), the agent still follows Procedure 1 and identifies TT, but also tries to find the true model for the current task from all candidate models, by ruling out the models that are very different with the current one. $u(c)$ is a model score of group $c \in \mathcal{C}$ which measures how possible c is the true model for the current task.

Compared with FMRL, FM-TempLe not only has lower sample complexity as proved in Section 5.2, but also saves computations due to the direct comparison of TTs.

Procedure 3 Finite-Model Template Learning (FM-TempLe)

Input: $\hat{\tau}; \epsilon; \gamma; m_s; m$ (same as Procedure 1);
 number of tasks in the first phase T_1 ; number of models C ;
 model error tolerance η

Output Near-optimal policies $\{\pi_t\}_{t=1,2,\dots}$

- 1: Initialize the TT group set \mathcal{G} , the TT visit set \mathcal{O} , and the MDP group set \mathcal{C} as empty
- 2: **for** $t \leftarrow 1, 2, \dots, T_1$ **do** ▷ Phase 1
- 3: Receive a task M_t , run Procedure 1 Line 3-20, and get visits $\mathbf{n}(s, a, \cdot)$ and $R(s, a), \forall (s, a) \in (\mathcal{S}, \mathcal{A})$
- 4: Cluster the past T_1 tasks into C groups (store in \mathcal{C}).
▷ model clustering
- 5: $\mathbf{g}_{(s,a,c)}, \sigma_{(s,a,c)} \leftarrow \text{GEN-TT}(\mathbf{n}_c(s, a), R_c(s, a)) \forall (s, a, c)$
- 6: **for** $t \leftarrow T_1 + 1, T_1 + 2, \dots$ **do** ▷ Phase 2
- 7: Receive a task M_t , do initializations as Line 3 in Procedure 1
- 8: Initialize model score $u(c) \leftarrow \eta, \forall c \in \mathcal{C}$
- 9: **for** $h \leftarrow 1, 2, \dots, H$ **do**
- 10: Run Procedure 1 Line 5-18, and get updated $\mathbf{n}(s_h, a_h, \cdot), R(s_h, a_h), \mathbf{g}_{(s_h, a_h)}, \sigma_{(s_h, a_h)}$
- 11: **if** $\|\mathbf{n}(s_h, a_h, \cdot)\|_{\ell_1} = m_s$ **then** ▷ TT is identified
- 12: **for** $c \in \mathcal{C}$ **do**
- 13: **if** $\mathbf{g}_{(s_h, a_h, c)} \neq \mathbf{g}_{(s_h, a_h)}$
or $\sigma_{(s_h, a_h, c)} \neq \sigma_{(s_h, a_h)}$ **then**
- 14: $u(c) \leftarrow u(c) - 1$ ▷ group identification
- 15: **if** \exists only 1 group $c^* \in \mathcal{C}$ s.t. $u(c^*) > 0$ **then**
- 16: AUGMENT($\mathbf{o}_{\mathbf{g}_{(s,a,c^*)}}, \mathbf{n}(s, a, \cdot), R(s, a), \sigma_{s,a}$)
▷ $\forall (s, a)$
- 17: Run Procedure 1 Line 19-20

5. Theoretical Analysis

This section provides sample complexity analysis of the proposed two algorithms O-TempLe and FM-TempLe (Procedure 1 and Procedure 3). Although O-TempLe and FM-TempLe can be applied to tasks with varying state/action spaces, we assume all tasks have the same \mathcal{S} and \mathcal{A} for

simplicity of notations, and the analysis extends to varying state/action spaces trivially.

We first make the following mild assumption, which is commonly used in RL (Jaksch et al., 2010), and it ensures the reachability of all state from any state on average.

Assumption 1. *There is a diameter D such that any state s' is reachable from any states s in at most D steps on average.*

Then, we define the underlying minimal distance among TTs as τ , namely TT gap; and define ν as the ranking gap, such that for any $\mathbf{g} \in \mathcal{G}$, if $\mathbf{g}_i^{(p)} > \mathbf{g}_j^{(p)}$ are two adjacent elements in $\mathbf{g}^{(p)}$, then either $\mathbf{g}_i^{(p)} - \mathbf{g}_j^{(p)} \geq \nu$, or $\mathbf{g}_i^{(p)} - \mathbf{g}_j^{(p)} \leq \mathcal{O}(\frac{\epsilon(1-\gamma)}{SV_{\max}})$. The ranking gap implies that for any s-a pair, the probabilities of transitioning to any two states are either very close, or substantially different. For simplicity, let ω denote $\max\{\min(\tau, \nu), \mathcal{O}(\frac{\epsilon(1-\gamma)}{\sqrt{SV_{\max}}})\}$.

5.1. Sample Complexity of O-TempLe

Theorem 3. *For any given $\epsilon > 0, 1 > \delta > 0$, running Procedure 1 on T tasks, each for at least $\tilde{\mathcal{O}}(\frac{DSA}{\omega^2})$ steps, generates at most*

$$\tilde{\mathcal{O}}\left(\frac{SGV_{\max}^3}{\epsilon^3(1-\gamma)^3} + \frac{TS AV_{\max}}{\omega^2 \epsilon(1-\gamma)}\right) \quad (1)$$

non- ϵ -optimal steps, with probability at least $1 - \delta$, where G is the total number of TTs.

Remark. (1) When ϵ is small, the sample complexity only has a linear dependence on the number of states S and the number of templates G , because the first term dominants. G is always no larger than $TS A$, and tends to be small in many cases. (2) When ϵ is not small and T is very large, the sample complexity has linear dependences on T, S and A since the second term dominants. (3) Our provided bound achieves the *lowest dependence on the environment size T, S, A* for MTRL, given that G is independent of T, S, A .

Proof Sketch. We first show that for any s-a pair, $m_s = \tilde{\mathcal{O}}(\frac{1}{\omega^2})$ samples would guarantee correct template identification and aggregation, and $m = \tilde{\mathcal{O}}(\frac{SV_{\max}^2}{\epsilon^2(1-\gamma)^2})$ samples are sufficient for estimating the s-a transition dynamics. Then we prove that all s-a pairs reach m_s within $H = \tilde{\mathcal{O}}(\frac{DSA}{\omega^2})$ steps. Finally, by computing the number of visits to unknown s-a pairs and applying the PAC-MDP theorem proposed by Strehl et al. (2012), we get the sample complexity result. The proof details are in Appendix C.

Comparison with a single-task learner. If sequentially run RMax for every task, the total sample complexity for T tasks is $\tilde{\mathcal{O}}\left(\frac{TS^2 AV_{\max}^3}{\epsilon^3(1-\gamma)^3}\right)$. (1) When ϵ is small, a significant improvement is achieved, since $\mathcal{O}(SG) \ll \mathcal{O}(TS^2 A)$. (2) When T is large, as long as $\frac{SV_{\max}^2}{\epsilon^2(1-\gamma)^2} \gg \frac{1}{\omega^2}$, our O-TempLe gains improved sample efficiency. (3) In the worst case,

$G = TSA$ (there is no similarity among all s-a transition dynamics) or $\omega^2 = \frac{SV_{\max}^2}{\epsilon^2(1-\gamma)^2}$, O-TempLe has the same-order sample complexity with RMax. Thus, O-TempLe will not cause negative transfer among tasks.

5.2. Sample Complexity of FM-TempLe

FM-TempLe works for the finite-model assumption, which is the same as FMRL (Brunskill & Li, 2013) and stated below.

Assumption 2. *There are at most C MDPs for all tasks, i.e., $|\mathcal{M}| \leq C$. Each task has at least $p_{\min} > 0$ task-prior probability to be drawn from \mathcal{M} .*

With this assumption, we derive the sample complexity of FM-TempLe.

Theorem 4. *For any given $\epsilon > 0, 1 > \delta > 0$, Procedure 3 on T tasks follows ϵ -optimal policies for all but*

$$\tilde{O}\left(\frac{SGV_{\max}^3}{\epsilon^3(1-\gamma)^3} + \frac{T_1 SAV_{\max}}{\omega^2 \epsilon(1-\gamma)} + \frac{(T-T_1)DC^2 V_{\max}}{\omega^2 \epsilon(1-\gamma)}\right) \quad (2)$$

steps with probability at least $1 - \delta$, where G is the total number of TTs, and

$$T_1 = \Omega\left(\frac{1}{p_{\min}} \ln \frac{C}{\delta}\right) \quad (3)$$

is the number of tasks in the first phase.

Remark. (1) When C is very large, or p_{\min} is very small, $T_1 \rightarrow T$ and FM-TempLe degenerates to O-TempLe. (2) If $DC^2 < SA$ and $T \gg T_1$, FM-TempLe requires fewer samples than O-TempLe.

Comparison with FMRL FM-TempLe has a large improvement over FMRL in most cases. The sample complexity of FMRL for T tasks in our notation is

$$\tilde{O}\left(\frac{CS^2 AV_{\max}^3}{\epsilon^3(1-\gamma)^3} + \frac{T_1 S^2 AV_{\max}^3}{\epsilon^3(1-\gamma)^3} + (T-T_1)\left(\frac{DC^2 V_{\max}}{\Gamma^2 \epsilon(1-\gamma)} + \frac{SCV_{\max}^3}{\epsilon^3(1-\gamma)^3}\right)\right). \quad (4)$$

where T_1 is the same as in Equation 3, and Γ is the model difference gap defined in Section 4 by Brunskill & Li (2013). We organize Equation 2 and Equation 4 both as three-term forms. The first term is for learning of all TTs or all models, where FM-TempLe reduces the dependence on S and gets rid of the dependence on A . The second term is for the first phase, and FMRL performs the same with a single-task RMax learner; FM-TempLe, by learning of templates, requires much fewer samples to get optimal policies. Finally, the last term is for the second phase. FMRL needs an additional model elimination step for each task, while FM-TempLe does not. FM-TempLe is worse than FMRL only in extreme cases where there are few MDP models with large model gaps, and a large number of TTs with small TT gaps or ranking gaps.

6. Experiments

In this section, we demonstrate empirical results of O-TempLe and FM-TempLe compared against the existing state-of-the-art algorithms. All experiments are conducted on a PC equipped with a 3.6 GHz INTEL CPU of 6 cores.

Setups. We define two domains, maze and gridworld, for online and finite-model settings respectively. Maze and gridworld are both grid environments with actions “up”, “down”, “left” and “right”. Three types of landforms, sand, marble and ice are used, with slipping probability 0, 0.2, 0.4 respectively. In a maze, the landform of every grid may be different, and the goal state is fixed for multiple tasks. In a gridworld, the landform is fixed for all grids, and the goal state varies for multiple tasks. So, under a certain number of grids S , the number of possible mazes is exponential in S whereas the number of possible gridworlds is linear in S .

Baselines. We choose the state-of-the-art MTRL algorithm, *Abstraction RL (Abs-RL)* (Abel et al., 2018) and *FMRL* (Brunskill & Li, 2013) as baselines. Abs-RL proposes multiple state abstraction types that can be combined with model-free methods such as Q-learning and Delayed-Q. We compare against “ ϕ_{Q^*} ”, “ $\phi_{Q^*_d}$ ”, and “ $\phi_{Q^*_e}$ ” combined with Q-learning, namely, “Abs- $\phi_{Q^*_e}$ ”, “Abs- $\phi_{Q^*_d}$ ”, and “Abs- ϕ_{Q^*} ”. Abs-RL is not PAC-MDP, so we could only compare with it empirically, not theoretically. Abs-RL works for both the online and finite-model setting, whereas FMRL works for the finite-model setting only. The base learners in FMRL, our O-TempLe and our FM-TempLe are chosen to be RMax (known threshold being 500) without loss of generality. Meanwhile, to show the effectiveness of our proposed algorithms and other MTRL algorithms, we also run RMax and Q-learning (Watkins & Dayan, 1992) individually for every single task without any knowledge transfer.

6.1. Results Under Different Settings

We design 3 groups of experiments with online tasks, finite-model tasks, and varying-sized environment tasks. The results are averaged over 20 runs.

Online MTRL. In the online setting, we consider 4×4 mazes with different arrangements of landforms streaming in. FMRL is not feasible in this setting as the types of underlying models is unknown and could be exponentially large. The threshold m_s is set to be 50, the number of episodes 3000, and the number of in-episode steps 30.

The per-task advantage rewards over single task RMax are displayed in Figure 3a. The cumulative rewards averaged across previous tasks are shown in Figure 3b. Among all agents, our O-TempLe obtains the highest average reward. We see during the first 40 tasks, the performance of O-TempLe continuously and rapidly grows by transferring previous knowledge. In contrast, the other agents do not

manage to learn from previous tasks as their performances do not show an increasing trend.

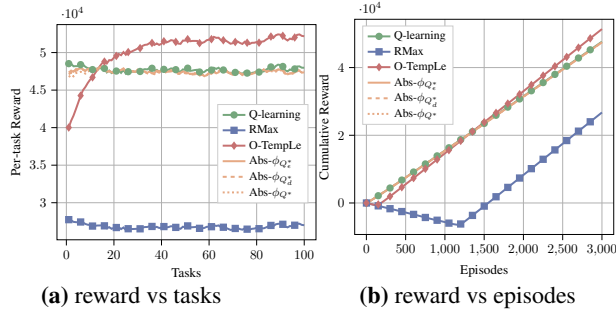


Figure 3. Online Setting: Performance of O-TempLe compared against RMax, Q-learning, Abs- $\phi_{Q_e^*}$, Abs- $\phi_{Q_d^*}$, and Abs- ϕ_{Q^*} on streaming-in mazes. The performance of Abs- $\phi_{Q_e^*}$, Abs- $\phi_{Q_d^*}$, and Abs- ϕ_{Q^*} are similar, thus overlapping curves.

Finite-Model MTRL. We generate two ice gridworlds with different goal states as the underlying models, and then randomly sample 50 tasks from the two underlying models. T_1 is set to be 15 for both FM-TempLe and FMRL.

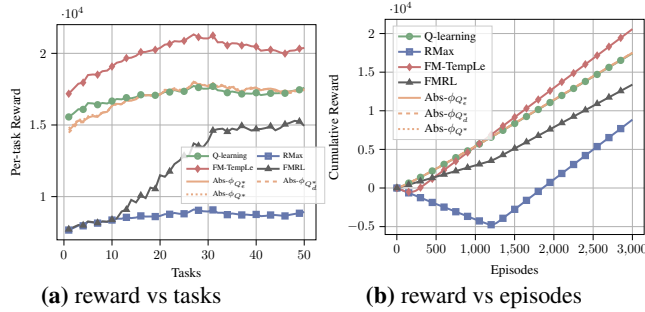
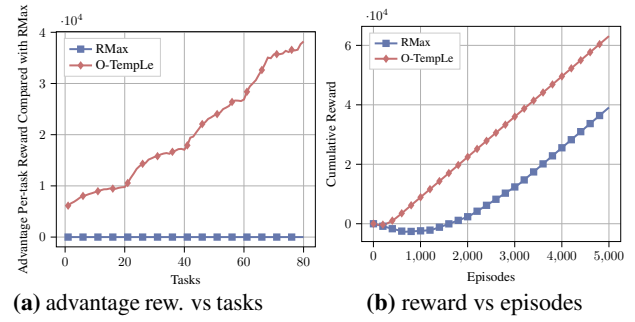


Figure 4. Finite-model Setting: Performance of FM-TempLe compared against FMRL, RMax, Q-learning, Abs- $\phi_{Q_e^*}$, Abs- $\phi_{Q_d^*}$, and Abs- ϕ_{Q^*} on 50 gridworlds with 2 underlying models.

Figure 4a and Figure 4b show the comparison of per-task rewards and average rewards. FMRL has the same performance with RMax in phase 1, and then achieves increasing rewards in the following tasks after successfully identify the underlying two types of MDPs. After 30 tasks, all state-actions pairs in the models become known, so the per-task reward converges. In contrast, FM-TempLe has a better start as it learns templates from the beginning. And model identification further helps with efficient learning. Over all tasks, FM-TempLe substantially outperforms other agents.

Varying Sized MTRL. We also test O-TempLe with multiple varying-sized mazes compared with single-task RMax since the other MTRL baselines are not feasible in this setting. We test O-TempLe’s ability to generalize knowledge learned in small tasks to speed up learning in larger tasks. Therefore, the first 20 tasks are 3×3 mazes, followed by 20 4×4 mazes, 20 5×5 mazes and 20 6×6 mazes. We show O-TempLe’s per-task advantage rewards over single task RMax in Figure 5a. The performance advantage over RMax increases over more observed tasks, verifying that O-

TempLe transfers knowledge among different-sized mazes.



(a) advantage rew. vs tasks **(b) reward vs episodes**

Figure 5. Varying Sized MTRL: Performance of O-TempLe compared with RMax and Q-learning on 80 varying-sized mazes.

6.2. Robustness of Hyper-parameters

TempLe requires a user-specified TT gap τ as input. Also, both FMRL and FM-TempLe require user-specified model gap Γ . We test the robustness of hyper-parameters to understand how significantly the performance of the algorithms could be affected by inaccurate guesses of τ and Γ , and show the results in Figure 6.

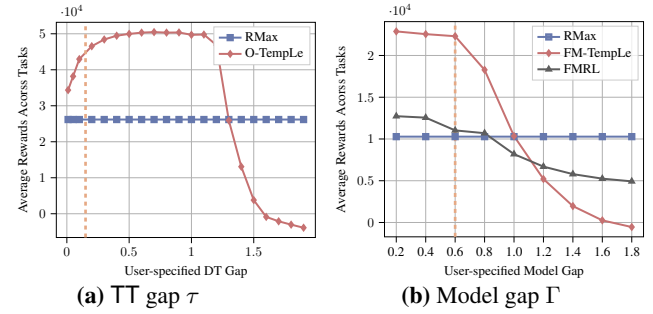


Figure 6. Hyper-parameter test of TT gap τ and model gap Γ , where the vertical dashed line shows the underlying true value.

According to Figure 6a, the performance of O-TempLe drops when τ is too large. However the rewards remain high for relatively small τ . Figure 6b shows that FM-TempLe gets higher reward than RMax when setting $\Gamma \leq 1$, although Γ has a larger influence on FM-TempLe compared to FMRL. Note that by definition, both τ and Γ would not exceed 1.8.

The results in Figure 6 guide the users to specify their TT gap and model gap when using TempLe. Interestingly, the best user-specified τ is slightly larger than the true τ , and the best user-specified Γ is slightly smaller than the true Γ , due to the trade-off between accuracy and efficiency.

7. Conclusion

In this work, we propose TempLe, the first PAC-MDP MTRL algorithm that works for tasks with varying state/action space. Two algorithms, O-TempLe and FM-TempLe, are introduced for online setting and finite-model setting respectively. We show in theory and experiments that O-TempLe and FM-TempLe both achieve higher sample efficiency than state-of-the-art methods.

References

- Abel, D., Arumugam, D., Lehnert, L., and Littman, M. State abstractions for lifelong reinforcement learning. In *International Conference on Machine Learning*, pp. 10–19, 2018.
- Ammar, H. B., Eaton, E., Luna, J. M., and Ruvolo, P. Autonomous cross-domain knowledge transfer in lifelong policy gradient reinforcement learning. In *Twenty-Fourth International Joint Conference on Artificial Intelligence*, 2015.
- Brafman, R. I. and Tennenholtz, M. R-max - a general polynomial time algorithm for near-optimal reinforcement learning. *J. Mach. Learn. Res.*, 3:213–231, March 2003. ISSN 1532-4435. URL <https://doi.org/10.1162/153244303765208377>.
- Brunskill, E. and Li, L. Sample complexity of multi-task reinforcement learning. *arXiv preprint arXiv:1309.6821*, 2013.
- Brunskill, E. and Li, L. Pac-inspired option discovery in lifelong reinforcement learning. In *International conference on machine learning*, pp. 316–324, 2014.
- Hayes, T. P. A large-deviation inequality for vector-valued martingales. *Combinatorics, Probability and Computing*, 2005.
- Jaksch, T., Ortner, R., and Auer, P. Near-optimal regret bounds for reinforcement learning. *Journal of Machine Learning Research*, 11(Apr):1563–1600, 2010.
- Kakade, S. M. et al. *On the sample complexity of reinforcement learning*. PhD thesis, University of London London, England, 2003.
- Kearns, M. and Singh, S. Near-optimal reinforcement learning in polynomial time. *Machine learning*, 49(2-3):209–232, 2002.
- Konidaris, G. and Barto, A. Autonomous shaping: Knowledge transfer in reinforcement learning. In *Proceedings of the 23rd international conference on Machine learning*, pp. 489–496, 2006.
- Li, S. and Zhang, C. An optimal online method of selecting source policies for reinforcement learning. In *Thirty-Second AAAI Conference on Artificial Intelligence*, 2018.
- Liu, Y., Guo, Z., and Brunskill, E. Pac continuous state online multitask reinforcement learning with identification. In *Proceedings of the 2016 International Conference on Autonomous Agents & Multiagent Systems*, pp. 438–446, 2016.
- Modi, A., Jiang, N., Singh, S., and Tewari, A. Markov decision processes with continuous side information. In *Algorithmic Learning Theory*, pp. 597–618, 2018.
- Ramamoorthy, S., Mahmud, M., Hawasly, M., and Rosman, B. Clustering markov decision processes for continual transfer. *School of Informatics, University of Edinburgh, Tech. Rep.*, 2013.
- Sharma, M., Holmes, M. P., Santamaría, J. C., Irani, A., Isbell Jr, C. L., and Ram, A. Transfer learning in real-time strategy games using hybrid cbr/rl. In *IJCAI*, volume 7, pp. 1041–1046, 2007.
- Strehl, A. L. and Littman, M. L. A theoretical analysis of model-based interval estimation. In *Proceedings of the 22Nd International Conference on Machine Learning, ICML '05*, pp. 856–863, New York, NY, USA, 2005. ACM. ISBN 1-59593-180-5. doi: 10.1145/1102351.1102459. URL <http://doi.acm.org/10.1145/1102351.1102459>.
- Strehl, A. L. and Littman, M. L. An analysis of model-based interval estimation for markov decision processes. *Journal of Computer and System Sciences*, 74(8):1309–1331, 2008.
- Strehl, A. L., Li, L., and Littman, M. L. Incremental model-based learners with formal learning-time guarantees. *arXiv preprint arXiv:1206.6870*, 2012.
- Taylor, M. E. and Stone, P. Representation transfer for reinforcement learning. In *AAAI Fall Symposium: Computational Approaches to Representation Change during Learning and Development*, pp. 78–85, 2007.
- Taylor, M. E. and Stone, P. Transfer learning for reinforcement learning domains: A survey. *Journal of Machine Learning Research*, 10(Jul):1633–1685, 2009.
- Torrey, L. and Shavlik, J. Transfer learning. In *Handbook of research on machine learning applications and trends: algorithms, methods, and techniques*, pp. 242–264. IGI Global, 2010.
- Watkins, C. J. and Dayan, P. Q-learning. *Machine learning*, 8(3-4):279–292, 1992.
- Wilson, A., Fern, A., Ray, S., and Tadepalli, P. Multi-task reinforcement learning: a hierarchical bayesian approach. In *Proceedings of the 24th international conference on Machine learning*, pp. 1015–1022. ACM, 2007.

Appendix: TempLe: Learning Template of Transitions for Sample Efficient Multi-task RL

A. Additional Definitions

Definition 5 (TT Gap). Define the TT distance between two TTs \mathbf{g}_a and \mathbf{g}_b as $\rho(\mathbf{g}_a, \mathbf{g}_b) = \|\mathbf{g}_a^{(p)} - \mathbf{g}_b^{(p)}\|_2 + |g_a^{(r)} - g_b^{(r)}|$. Suppose there is a minimum TT distance τ , such that for any two different TTs $\mathbf{g}_a, \mathbf{g}_b \in \mathcal{G}$, $\rho(\mathbf{g}_a, \mathbf{g}_b) \geq \tau$. We name τ as TT gap.

The permutation from an s-a transition dynamics to a TT is recorded by a ranking permutation defined as below.

Definition 6 (Ranking Permutation). For an s-a pair (s, a) with transition probability vector $\mathbf{p} \in \mathbb{R}^S$ where $p_i = p(s_i | s, a)$, by sorting its elements from the largest to the smallest value, we get an ordered vector $\mathbf{g}^{(p)}$. Define function $\sigma : \{1, \dots, S\} \rightarrow \{1, \dots, S\}$ as a mapping from ranking to the indices in \mathbf{p} . For example, $\sigma(i)$ is the index of the i -th largest element of \mathbf{p} , i.e., $\mathbf{g}_i^{(p)} = \mathbf{p}_{\sigma(i)}$. The inverse function σ^{-1} maps indices to ranking. So $\sigma^{-1}(j)$ is the ranking of \mathbf{p}_j , i.e., $\mathbf{g}_{\sigma^{-1}(j)}^{(p)} = \mathbf{p}_j$. The way way? ordering is unique if for any $\mathbf{p}_i = \mathbf{p}_j$ and $i < j$, we put \mathbf{p}_i before \mathbf{p}_j in $\mathbf{g}^{(p)}$. As a result, $\sigma(\cdot)$ is a bijection and can be regarded as a permutation. We call it **ranking permutation** of (s, a) .

For simplicity, we slightly abuse notation and use $\sigma(\mathbf{p})$ to denote the re-ordered vector. Thus $\mathbf{g}^{(p)} = \sigma(\mathbf{p})$ and $\mathbf{p} = \sigma^{-1}(\mathbf{g}^{(p)})$.

Definition 7 (Ranking Gap). Define ν as the minimal notable ranking gap, such that for any $\mathbf{g} \in \mathcal{G}$, if $\mathbf{g}_i^{(p)} > \mathbf{g}_j^{(p)}$ are two adjacent elements in $\mathbf{g}^{(p)}$ and $\mathbf{g}_i^{(p)} - \mathbf{g}_j^{(p)} \geq \mathcal{O}(\frac{\epsilon(1-\gamma)}{SV_{\max}})$, then $\mathbf{g}_i^{(p)} - \mathbf{g}_j^{(p)} \geq \nu$ holds. In other words, two adjacent elements of $\mathbf{g}^{(p)}$ satisfy either $\mathbf{g}_i^{(p)} - \mathbf{g}_j^{(p)} \geq \nu$ or $\mathbf{g}_i^{(p)} - \mathbf{g}_j^{(p)} \leq \mathcal{O}(\frac{\epsilon(1-\gamma)}{SV_{\max}})$.

If two adjacent elements are different by no more than $\mathcal{O}(\frac{\epsilon(1-\gamma)}{SV_{\max}})$, then the corruption can be ignored because it will not influence the value of the policy too much, as proved in Lemma 12. Otherwise we need adequate samples to make sure the ranking of elements will succeed.

B. An Intuitive Example Illustrating Sample Efficiency of Our Algorithm

We use the gridworld in Figure 2 as an example to illustrate how the augmented estimation saves samples by estimating TTs instead of every s-a pairs. For simplicity, we assume the possibility of arbitrarily sampling any s-a pair and observing its transitions. The gridworld in Figure 2 has 100 distinct s-a transition dynamics, but only 2 distinct TTs. The distance between the 2 TTs is 0.28.

The objective is to estimate $p(s, a)$ such that $\|\hat{p}(s, a) - p(s, a)\| \leq 0.01$ for all (s, a) with probability 95%. Using the conventional estimation, the total number of samples we need is² $\mathcal{O}(100 \times \frac{1}{0.01^2} \ln \frac{100}{0.05}) \approx 7.6 \times 10^6$. However our proposed augmented estimation only requires $\sim 1.25\%$ of samples needed by the conventional estimation, since it takes $\mathcal{O}(100 \times \frac{1}{0.28^2} \ln \frac{100}{0.025}) \approx 1.1 \times 10^4$ samples to correctly identify the TTs of all s-a pairs with probability $1 - \delta/2$, plus $\mathcal{O}(2 \times \frac{1}{0.01^2} \ln \frac{2}{0.025}) \approx 8.4 \times 10^4$ samples to get 0.01-accurate estimations of 2 TTs with probability $1 - \delta/2$.

C. Proofs of Main Theorems

C.1. Proof of Theorem 3

To prove Theorem 3, we first present Lemma 8, Lemma 10, Lemma 11, Lemma 12 and Lemma 13.

Lemma 8 and Lemma 10 provide the sample size requirements for correctly identifying the TT of an s-a pair.

Lemma 8. For any state-action pair, suppose the ranking permutation of the estimated probability vector is the same with that of the underlying probability vector, then it would be identified to its corresponding TT group correctly with $\mathcal{O}(\frac{1}{\tau^2} \ln \frac{1}{\delta})$ samples, with probability at least $1 - \delta$, where τ is the TT gap defined in Definition 5.

Proof. For an state-action pair (s, a) , define the observation vector of the i th sample as $Z_i = [\mathbb{I}_{s'=s_1}, \mathbb{I}_{s'=s_2}, \dots, \mathbb{I}_{s'=s_S}, r]$.

²According to Hoeffding's inequality, $\mathcal{O}(\frac{1}{\alpha^2} \ln \frac{1}{\delta})$ samples are needed to achieve an α -accurate estimation with probability $1 - \delta$.

Define $X_n = \sum_{i=1}^n Z_i - n\theta(s, a)$, and set $X_0 = 0$.

We first prove the sequence $\{X_n\}$ is a vector-valued martingale.

$$\begin{aligned} E(X_n | X_0, X_1, \dots, X_{n-1}) &= E\left[\sum_{i=1}^n Z_i - n\theta(s, a) | X_0, X_1, \dots, X_{n-1}\right] \\ &= E\left[\sum_{i=1}^{n-1} Z_i - (n-1)\theta(s, a) + Z_n - \theta(s, a) | X_0, X_1, \dots, X_{n-1}\right] \\ &= X_{n-1} + E[Z_n - \theta(s, a)] \\ &= X_{n-1} \end{aligned}$$

Obviously, $E[\|X_n\|] < \infty$ for all n . Thus $\{X_n\}$ is a (strong) martingale.

By application of the extended Hoeffding's inequality (Hayes, 2005), we get

$$Pr\left(\left\|\frac{1}{n}\sum_{i=1}^n Z_i - \theta(s, a)\right\| \geq \epsilon\right) \leq 2e^{2 - \frac{n\epsilon^2}{2}}$$

Set the failure probability as δ , we obtain $n \geq \mathcal{O}\left(\frac{1}{\epsilon^2} \ln \frac{1}{\delta}\right)$. □

Lemma 8 assumes perfect permutation, and Lemma 10 addresses the problem of how to avoid notable corruptions of permutations. For ease of illustrating, we define the concept *almost the same* and *almost correct* in Definition 9.

Definition 9 (Almost the same and almost correct). *If for two probability vectors p and p' , their ranking permutations σ and σ' are the same except for elements whose difference is smaller than $\mathcal{O}\left(\frac{\epsilon(1-\gamma)}{SV_{\max}}\right)$, then we call σ and σ' almost the same. If p' is the approximation of the ground truth p , then we call σ' almost correct.*

Lemma 10. *With $\tilde{\mathcal{O}}\left(\frac{1}{\nu^2} \ln \frac{S}{\delta}\right)$ samples of a s-a pair, its transition permutation will be almost correct, with probability $1 - \delta$.*

Proof. Suppose there is a transition probability vector p with length l , as well as transition-difference gap ν . We estimate p by randomly sampling indices $1, \dots, i, \dots, l$ according to the probability distribution p . Let $\hat{p} = \left[\frac{n(1)}{n}, \dots, \frac{n(l)}{n}\right]$.

For any two adjacent elements p_i and p_j (adjacent means there is no p_k whose value is between p_i and p_j), we want our estimations $\frac{n(i)}{n}$ and $\frac{n(j)}{n}$ to satisfy $\frac{n(i)}{n} > \frac{n(j)}{n}$. It is sufficient if we guarantee $\frac{n(i)}{n}$ and $\frac{n(j)}{n}$ are respectively $\nu/2$ -close to p_i and p_j . By Hoeffding's inequality,

$$P\left(\left|\frac{n(i)}{n} - p_i\right| > \frac{\nu}{2}\right) \leq 2 \exp(-2n(\nu/2)^2)$$

Therefore, $n \geq \mathcal{O}\left(\frac{1}{\nu^2} \ln \frac{1}{\delta}\right)$ is sufficient. By union bound, we have $n \geq \mathcal{O}\left(\frac{1}{\nu^2} \ln \frac{S}{\delta}\right)$. □

Lemma 8 and Lemma 10 imply that the small threshold should satisfy $m_s = \tilde{\mathcal{O}}\left(\frac{1}{\min\{\tau^2, \nu^2\}}\right)$.

Then, Lemma 11 claims if horizon is set to be large enough, all s-a pairs will have sufficient samples to be correctly grouped.

Lemma 11. *If $H = \tilde{\mathcal{O}}\left(\frac{D SA}{\omega^2}\right)$, all state-action pairs in the task will have at least $\tilde{\mathcal{O}}\left(\frac{1}{\omega^2} \ln \frac{T SA}{\delta}\right)$ samples with probability $1 - \delta$.*

The proof of Lemma 11 is similar to Lemma 2.1 in paper (Brunskill & Li, 2013).

Lemma 12 is a variant of the ‘‘simulation lemma’’ (Kearns & Singh, 2002; Brafman & Tennenholtz, 2003) with TT estimation.

Lemma 12. *For any two MDPs M and \tilde{M} with the same $\mathcal{S}, \mathcal{A}, \mu, \gamma$, if for any s-a pair (s, a) , the ranking permutations of $p(s, a)$ and $\tilde{p}(s, a)$ are almost the same, and $\mathbf{g} = (\text{desc}(p(s, a)), r(s, a))$ as well as $\tilde{\mathbf{g}} = (\text{desc}(\tilde{p}(s, a)), \tilde{r}(s, a))$ satisfy $\|\mathbf{g}^{(p)} - \tilde{\mathbf{g}}^{(p)}\| \leq \mathcal{O}\left(\frac{\epsilon(1-\gamma)}{V_{\max}}\right)$ and $|g^{(r)} - \tilde{g}^{(r)}| \leq \mathcal{O}\left(\frac{\epsilon(1-\gamma)}{V_{\max}}\right)$, then for any policy π , $|V_M^\pi - V_{\tilde{M}}^\pi| \leq \epsilon$.*

Proof. For an s-a pair (s, a) , suppose its ranking permutation in M is σ , and the ranking permutation in \tilde{M} is $\tilde{\sigma}$.

We first assume σ and $\tilde{\sigma}$ are exactly the same. So we have $\mathbf{g}^{(p)} = \sigma(p(s, a))$ and $\tilde{\mathbf{g}}^{(p)} = \sigma(\tilde{p}(s, a))$.

Thus $\|\mathbf{g}^{(p)} - \tilde{\mathbf{g}}^{(p)}\| \leq \mathcal{O}(\frac{\epsilon(1-\gamma)}{V_{\max}})$ implies $\|p(s, a) - \tilde{p}(s, a)\| \leq \mathcal{O}(\frac{\epsilon(1-\gamma)}{V_{\max}})$, because of the property of permutation.

Similarly, $|g^{(r)} - \tilde{g}^{(r)}| \leq \mathcal{O}(\frac{\epsilon(1-\gamma)}{V_{\max}})$ implies $|r(s, a) - \tilde{r}(s, a)| \leq \mathcal{O}(\frac{\epsilon(1-\gamma)}{V_{\max}})$.

Then, following the standard proof (Strehl & Littman, 2008; Strehl et al., 2012), it is easy to show $|V_M^\pi - V_M^\pi| \leq \epsilon$.

Next, we allow σ and $\tilde{\sigma}$ be almost the same (see Definition 9), and show that it only causes up to a constant factor increase in the value difference $|V_M^\pi - V_M^\pi|$.

Without loss of generality, assume $\tilde{\sigma}$ only reverses σ in indices i and j , i.e., $\sigma(i) = \tilde{\sigma}(j)$ and $\sigma(j) = \tilde{\sigma}(i)$. According to the definition of almost the same, $p_{\sigma(i)} - p_{\sigma(j)} = p_{\tilde{\sigma}(j)} - p_{\tilde{\sigma}(i)} \leq \mathcal{O}(\frac{\epsilon(1-\gamma)}{SV_{\max}})$. Then we have

$$\begin{aligned} \|p(s, a) - \tilde{p}(s, a)\| &= \|\sigma^{-1}(\mathbf{g}^{(p)}) - \tilde{\sigma}^{-1}(\tilde{\mathbf{g}}^{(p)})\| \\ &= |g_1^{(p)} - \tilde{g}_1^{(p)}| + \dots + |g_i^{(p)} - \tilde{g}_j^{(p)}| + |g_j^{(p)} - \tilde{g}_i^{(p)}| + \dots + |g_S^{(p)} - \tilde{g}_S^{(p)}| \\ &\leq \|\mathbf{g}^{(p)} - \tilde{\mathbf{g}}^{(p)}\| + |g_i^{(p)} - \tilde{g}_j^{(p)}| + |g_j^{(p)} - \tilde{g}_i^{(p)}| \\ &\leq \mathcal{O}(\frac{\epsilon(1-\gamma)}{V_{\max}}) + \mathcal{O}(\frac{2\epsilon(1-\gamma)}{SV_{\max}}) \\ &\leq (1 + \frac{2}{S})\mathcal{O}(\frac{\epsilon(1-\gamma)}{V_{\max}}) \end{aligned}$$

Therefore, if $\tilde{\sigma}$ differs with σ in all indices, as long as they are almost the same, $|V_M^\pi - V_M^\pi| \leq 2\epsilon$. By adjusting the constant factor, $|V_M^\pi - V_M^\pi| \leq \epsilon$ also holds. \square

According to Lemma 12, if each TT gets $\mathcal{O}(\frac{\epsilon(1-\gamma)}{V_{\max}})$ -accurate estimation, then all the s-a transition dynamics associated with the same TT will be accurate enough to generate an ϵ -optimal policy. Therefore, the regular known threshold m is still the same as in RMax, i.e., $m = \tilde{\mathcal{O}}(\frac{SV_{\max}^2}{\epsilon^2(1-\gamma)^2})$. Note that the small threshold should not exceed the regular threshold, so $m_s = \tilde{\mathcal{O}}(\frac{1}{\omega^2})$, where $\omega = \max\{\min(\tau, \nu), \mathcal{O}(\frac{\epsilon(1-\gamma)}{\sqrt{SV_{\max}}})\}$. If τ or ν is smaller than $\mathcal{O}(\frac{\epsilon(1-\gamma)}{\sqrt{SV_{\max}}})$, then the small threshold becomes the regular threshold and O-TempLe degenerates to RMax.

Next, we show in Lemma 13 the total number of visits to unknown state-action pairs during T tasks.

Lemma 13. *The total number of visits to unknown s-a pairs during the execution of Algorithm 1 for T tasks is*

$$\tilde{\mathcal{O}}\left(\frac{TSA}{\omega^2} + \frac{SGV_{\max}^2}{\epsilon^2(1-\gamma)^2}\right) \quad (5)$$

Proof. For every task, Algorithm 1 first uses known threshold $m_s = \tilde{\mathcal{O}}(\frac{1}{\omega^2})$ for all s-a pairs. And the first m_s visits to an s-a pair are all visits to unknowns. So all the SA s-a pairs over T tasks take $\mathcal{O}(\frac{TSA}{\omega^2})$ steps of visiting unknowns in total.

Once an s-a pair is roughly known (having visits more than m_s), the TT is identified, and the known threshold is changed to m for the s-a pair. If the corresponding TT is fully known (having visits more than m), then the s-a pair immediately becomes fully known by incorporating all visit counts of the TT. If the corresponding TT is not fully known yet, visits to the s-a pair are still counted as visits to unknown, until the TT is known. Therefore, for every possible TT, there are m unknown visits. And G TTs result in Gm unknown visits, which is the second term in Equation 5 \square

Now we can proceed to prove the main theorem.

Proof. (of Theorem 3) We apply the PAC-MDP theorem proposed by (Strehl et al., 2012) to get the sample complexity of O-TempLe. Proposition 1 in (Strehl et al., 2012) claims that any greedy learning algorithm with known set K and known state-action MDP M_K satisfies 3 conditions (optimism, accuracy and learning complexity) will follow a 4ϵ -optimal policy on all but $\mathcal{O}\left(\frac{V_{\max}}{\epsilon(1-\gamma)} \ln \frac{1}{\delta} \ln \frac{1}{\epsilon(1-\gamma)}\right)$ timesteps with probability $1 - 2\delta$, where $\zeta(\epsilon, \delta)$ is the total number of updates of action-value estimates plus the number of visits to unknowns. This proposition, though focuses on single-task learners, can be easily adapted to work for multi-task learners, as shown in (Brunskill & Li, 2013).

Now we verify that the required 3 conditions all hold for our algorithm.

(1) $Q_t(s, a) \geq Q^*(s, a) - \epsilon$ for any timestep t (optimism).

This condition naturally holds as the single-task learner RMax chooses actions by optimistic value functions. O-TempLe does not change the way of choosing actions. It is similar for using E^3 or MBIE as the single-task learner.

(2) $V_t(s) - V_{M_{K_t}}^{\pi_t}(s) \leq \epsilon$ for any timestep t (accuracy).

An s-a pair is in M_K if it is fully known, i.e., $n(s, a) \geq m$. A part of $n(s, a)$ may come from the visits to other s-a pairs with the same TT. According to Lemma 12, condition (2) holds if the estimation of the TT is within $\mathcal{O}(\frac{\epsilon(1-\gamma)}{V_{\max}})$ accuracy. By Hoeffding's inequality, to achieve this accuracy, $m = \frac{SV_{\max}^2}{\epsilon^2(1-\gamma)^2}$ samples are required for a TT.

(3) The total number of updates of action-value estimates plus the number of visits to unknowns is bounded by $\zeta(\epsilon, \delta)$ (learning complexity).

Lemma 13 already gives the number of visits to unknown s-a pairs, and the updates of action-value estimates will happen no more than TSA times for T tasks. Hence, $\zeta(\epsilon, \delta) = \tilde{\mathcal{O}}\left(\frac{TSA}{\omega^2} + \frac{SGV_{\max}^2}{\epsilon^2(1-\gamma)^2}\right)$.

Therefore, the sample complexity of O-TempLe is

$$\tilde{\mathcal{O}}\left(\left(\frac{TSA}{\omega^2} + \frac{SGV_{\max}^2}{\epsilon^2(1-\gamma)^2}\right) \left(\frac{V_{\max}}{\epsilon(1-\gamma)} \ln \frac{1}{\delta} \ln \frac{1}{\epsilon(1-\gamma)}\right)\right)$$

□

C.2. Proof of Theorem 4

Proof. (of Theorem 4)

The proof of Theorem 4 is similar to the proof of Theorem 3, because FM-TempLe is adapted from O-TempLe. The only difference lies in the number of visits to unknown s-a pairs.

In the first phase, FM-TempLe is the same with O-TempLe, so the number of visits to identify TTs is $\tilde{\mathcal{O}}(\frac{T_1SA}{\omega^2})$.

In the second phase, FM-TempLe avoids visiting all s-a pairs for at least m_s times under the help of finite models. As (Brunskill & Li, 2013) shows, we need at most C^2 informative s-a pairs to fully identify a model, where an s-a pair is ‘‘informative’’ if at least two MDP models have sufficient disagreement in its dynamics. Similarly with Lemma 11, $\tilde{\mathcal{O}}(\frac{DC^2}{\omega^2})$ samples are enough to let all these C^2 informative s-a pairs roughly known. Then the correct model for the current task would be identified. Thus, for every task in the second phase, $\tilde{\mathcal{O}}(\frac{DC^2}{\omega^2})$ visits to unknowns are needed.

Finally, for each TT, its visits are shared among s-a pairs and tasks, no matter which phase they are in. Hence there are still $\tilde{\mathcal{O}}(\frac{SGV_{\max}^3}{\omega^2\epsilon(1-\gamma)})$ visits to unknowns.

Adding the above three parts of visits to unknowns, and following the proof of Theorem 3, we obtain the sample complexity of Theorem 4.

□